Neuron, Vol. 35, 681–696, August 15, 2002, Copyright ©2002 by Cell Press

Minigenes Impart Odorant Receptor-Specific Axon Guidance in the Olfactory Bulb

Anne Vassalli,[1] Andrea Rothman, Paul Feinstein, Martin Zapotocky, and Peter Mombaerts[1]
The Rockefeller University
1230 York Avenue
New York, New York 10021

Summary

An olfactory sensory neuron (OSN) expresses selectively one member from a repertoire of ~1000 odorant receptor (OR) genes and projects its axon to a specific glomerulus in the olfactory bulb. Both processes are here recapitulated by *MOR23* and *M71* OR minigenes, introduced into mice. Minigenes of 9 kb and as short as 2.2 kb are selectively expressed by neurons that do not coexpress the endogenous gene but coproject their axons to the same glomeruli. Deletion of a 395 bp upstream region in the *MOR23* minigene abolishes expression. In this region we recognize sequence motifs conserved in many OR genes. Transgenic lines expressing the OR in ectopic epithelial zones form ectopic glomeruli, which also receive input from OSNs expressing the cognate endogenous receptor. This suggests a recruitment through homotypic interactions between OSNs expressing the same OR.

Introduction

The mammalian nose detects odorous chemicals using odorant receptors (ORs) (Buck and Axel, 1991; Buck, 2000). ORs are seven-transmembrane domain proteins expressed on the cilia of olfactory sensory neurons (OSNs) within the olfactory epithelium. OR genes form the largest families in vertebrate genomes, consisting of ~1000 members in mouse and human (Mombaerts, 2001a; Zhang and Firestein, 2002). An individual OSN expresses a single OR gene at a high level ("monogenic" expression) (Malnic et al., 1999; Touhara et al., 1999; Bozza et al., 2002). Moreover, only one allele is expressed per OSN (Chess et al., 1994; Ishii et al., 2001). Together, these properties of monogenic and monoallelic expression define "singular" expression. A given OR is expressed in a small subset of OSNs whose cell bodies are scattered within one of four zones of the epithelium (Ressler et al., 1993; Vassar et al., 1993). Axons of OSNs expressing the same OR converge to glomeruli in the olfactory bulb, as shown by in situ hybridization (Ressler et al., 1994; Vassar et al., 1994) and targeted mutagenesis (Mombaerts et al., 1996). In addition to their role as receptors for odorous ligands, ORs have an instructive role but are not the sole determinants in the guidance of axons to their glomerulus (Mombaerts et al., 1996; Wang et al., 1998). The concept of the glomerulus as a site of axonal convergence for one OR type suggests that odor quality is encoded by a specific combination of activated glomeruli. Thus, the related processes of OR gene choice and glomerular convergence are central to the functional organization of olfactory perception (Mombaerts, 2001b).

The mechanisms underlying OR gene choice and expression remain enigmatic. Sequence inspection and comparison of human and mouse OR loci (Tsuboi et al., 1999; Bulger et al., 2000; Hoppe et al., 2000; Sosinsky et al., 2000; Lane et al., 2001) have identified a number of motifs upstream of the putative start sites of transcription with various degrees of conservation. These analyses were however not based on experimental evidence from transfection or transgenesis, and no coherent picture has emerged. Experimental investigations in transgenic mice (Qasba and Reed, 1998; Ebrahimi et al., 2000; Serizawa et al., 2000; Ishii et al., 2001) have not yielded consistent results: it has not been resolved if OR gene expression is under short-range control (Qasba and Reed, 1998) or is governed by long-range elements (Serizawa et al., 2000).

How does one determine that the "correct" expression pattern has been reproduced in transgenic mice? An OR transgene is not expressed in the same cells as its endogenous OR counterpart but is expressed in a mutually exclusive fashion (Serizawa et al., 2000). A stringent indicator that the correct expression pattern has been achieved is glomerular coconvergence of axons of OSNs that express the OR from the transgene, together with axons of OSNs that express the same OR from the endogenous locus. Because neuronal identity is critically dependent on the specificity of the expressed OR (Mombaerts et al., 1996; Wang et al., 1998), glomerular coconvergence is a measure of the recapitulation by the transgene of the phenotypic identity of OSNs expressing the endogenous OR gene.

Here, we define functional units of expression, or "minigenes," for two mouse OR genes that belong to different gene clusters: *MOR23* (Asai et al., 1996) and *M71* (Ressler et al., 1994). For both genes, genomic segments of ~9 kb are able to impart an expression pattern paralleling that of the endogenous genes: transgene expression is OSN specific, punctate, restricted to the correct zone, and likely singular. Shown for the first time, it is associated with axonal projection to the cognate glomeruli. The shortest *MOR23* minigene featuring glomerular coconvergence with the endogenous *MOR23* gene is 2.2 kb long.

We also find that transgenic lines having aberrant zonal expression exhibit correlated changes in their axonal projections to the olfactory bulb. The mistargeting of transgene-expressing OSNs is accompanied by mistargeting of a fraction of the OSNs expressing the endogenous gene to the same ectopic glomeruli. We propose that the combination of an expressed OR and a zone of expression specifies discrete loci of convergence in the olfactory bulb and that homotypic interactions between OSNs expressing a same OR have a role in elaborating the topography of axonal projections.

[1]Correspondence: peter@rockefeller.edu (P.M.), vassala@rockefeller.edu (A.V.)

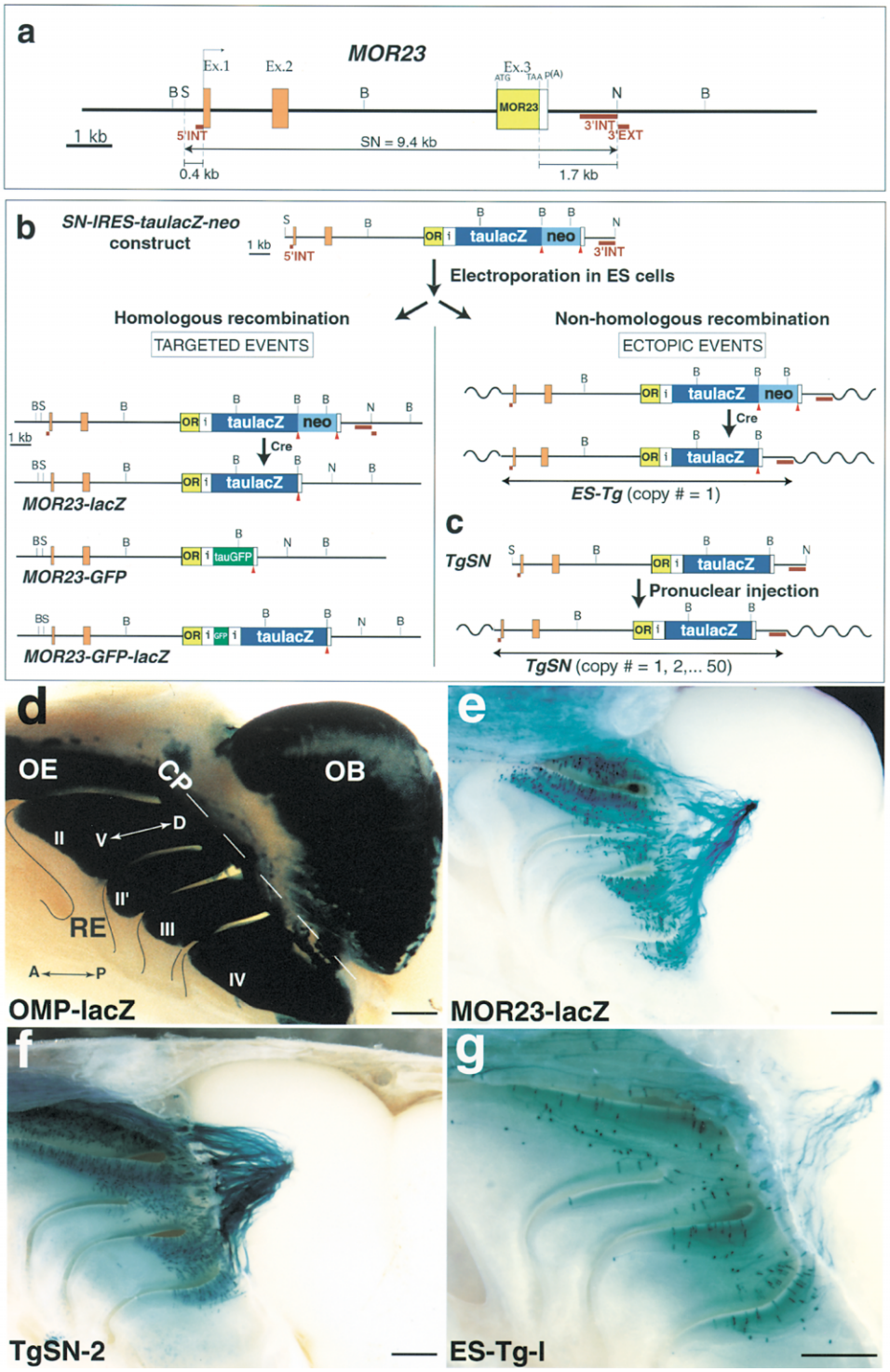

Figure 1. Structure, Targeted Mutagenesis, and Transgenesis of the *MOR23* Gene

(a) The *MOR23* gene, with its three-exon structure defined by 5′RACE analysis of C57BL/6J mouse RNA. The putative TSS (hooked arrow) is located at position 1618 in GenBank X92969. Two exons (orange boxes), of 154 bp and 349 bp, respectively, are present in the 5′ noncoding region. The introns span 1.4 and 4.5 kb, respectively. The coding region (930 bp, yellow box) is encoded within a single exon containing 16 bp of 5′ noncoding sequence. The 3′ noncoding region (white box) is shown to extend to a unique polyadenylation signal found within a 1.7 kb region downstream of the stop codon. This 3′ noncoding region contains putative donor and acceptor splice sites, defining a hypothetical ~100 bp intron. The 9.4 kb SacI-NheI (SN) fragment is the substrate for targeting vector and transgene construction. Red bars represent the probes used in genomic Southern blots: 5′INT, 3′INT, used as 5′ and 3′ internal probes, respectively, of the SN fragment; 3′EXT, probe external to the SN fragment, used to identify targeted ES clones. B, BamHI; N, NheI; S, SacI.

(b) Production of gene-targeted and transgenic mice. The targeting construct was electroporated into ES cells. Southern blot analysis of

Results

The *MOR23* and *M71* OR Genes

The *MOR23* gene (Asai et al., 1996) is a member of a cluster of at least 19 OR genes located at the distal end of chromosome 1 (*Olfr16*). It is separated from its OR gene neighbors by ~650 kb upstream and 90 kb downstream (Celera database). Among these genes is the closest homolog of *MOR23*, with 69% amino acid identity. The *M71* gene (Ressler et al., 1994) belongs to the *Olfr7* cluster on chromosome 9, comprising ~100 OR genes (Sullivan et al., 1996; Xie et al., 2000). The *M71* gene is positioned between the *K22* and *M72* genes at a distance of 15 and 26 kb, respectively. *M72* is the closest homolog of *M71*, with 96% amino acid identity, and appears to define the centromeric end of the *Olfr7* cluster. The expression of the *MOR23* and *M71* genes overlap within the most dorsomedial zone of the olfactory epithelium, "zone 4" in the nomenclature of Vassar et al. (1993). However, axons of OSNs expressing either gene converge to glomeruli that reside at considerable distances from each other in each hemisphere of the olfactory bulb.

We determined the structure of these two OR genes by rapid amplification of 5′ cDNA ends (5′ RACE) analysis of olfactory mucosa RNA. The 5′-most RACE products define the putative transcription start sites (TSS). The *MOR23* gene consists of two upstream noncoding exons and a third exon containing the entire 930 bp coding region (Figure 1a). The *M71* gene has one upstream noncoding exon (Figure 4a). An ~9 kb genomic segment was chosen for either OR gene to be tested for autonomous function in transgenic mice.

Reference Expression Pattern of *MOR23*

To provide a reference for the *MOR23* transgenic lines, we tagged the endogenous *MOR23* gene by homologous recombination (Figure 1b) with an *IRES-taulacZ* cassette (MOR23-lacZ strain), an *IRES-tauGFP* cassette (MOR23-GFP strain), or an *IRES-GFP-IRES-taulacZ* cassette (MOR23-GFP-lacZ strain). The *IRES* sequence allows for coexpression of the OR with a histological marker. Examination of whole-mount specimens (Figures 1e and 2d) and sections (data not shown) indicates that expression is in zone 4 (compare to Figures 1d and 2a for views of the entire olfactory epithelium). A single labeled glomerulus is seen in both the medial (Figure 1e) and lateral hemispheres of each bulb. Thus, there are four labeled glomeruli per mouse.

To show that genetic manipulation of the *MOR23* gene does not alter the targets of axonal projections of OSNs that express it, we sectioned MOR23-GFP heterozygous and homozygous bulbs. We observed that heterozygous glomeruli contain a mixture of GFP-negative and GFP-positive axons, whereas homozygous glomeruli are fully GFP positive (Figure 3f). The most likely interpretation of this pattern is that MOR23-GFP-expressing OSNs innervate the same glomeruli as OSNs expressing the wild-type, unmodified *MOR23* gene.

To verify monoallelic expression, individual OSNs of MOR23-lacZ/MOR23-GFP compound heterozygous mice were examined using antibodies to β-galactosidase (red) and GFP fluorescence (Rodriguez et al., 1999). Among 1292 labeled OSNs from three mice, none were doubly labeled: 642 (49.7%) were red, and 650 (50.3%) were green (Figure 3a). As a control for our ability to detect doubly labeled cells, red and green fluorescent signals were demonstrated to coincide at the level of individual OSNs of MOR23-GFP-lacZ mice (Figure 3b). Stained glomeruli of MOR23-lacZ/MOR23-GFP mice are doubly labeled (Figure 3g), reflecting the glomerular coconvergence of axons from these two distinct OSN populations.

MOR23 Transgenic Mice

A 9.4 kb SacI-NheI *MOR23* genomic fragment (abbreviated SN) was used to build the transgene (Figure 1a). This sequence includes 0.4 kb upstream of the putative TSS and 1.7 kb downstream of the coding region. Two different methods for inserting DNA ectopically into the germline of mice were used, as various modes of transgene delivery may sample distinct regions of the genome. First, the transgene was introduced into ES cells by electroporation, and clones were selected for *neo* expression (Figure 1b). Second, a version of the transgene devoid of the *neo*-selectable marker was microinjected into the pronuclei of one-cell embryos (Figure 1c).

MOR23 gene targeting experiments yielded hundreds of nonhomologous recombinants that were screened for single-copy ectopic integration of the targeting vector and integrity at its 5′ and 3′ ends. The *SN-IRES-taulacZ-neo* construct generated three mouse lines, two

G418-resistant ES cell clones identified homologous (targeted) and nonhomologous (ectopic) recombination events. Three gene-targeted mutations were generated with different cassettes. Ectopic events were further screened for single-copy (n = 1) integration of a full-length transgene, using the 5′INT and 3′INT probes. Cre-mediated site-specific recombination served in both cases to excise the *neo* selectable marker; the red triangles flanking the *neo* gene are *loxP* sites. OR, *MOR23* coding sequence; i, *IRES*.

(c) A second series of transgenic lines was generated by microinjection of the SN construct into one-cell embryos, resulting in transgenic strains (TgSN) that carry one or frequently several transgene copies.

(d–g) Expression patterns in MOR23-lacZ targeted and SN transgenic mice. Whole-mount preparations of sagitally transected mouse heads, showing the medial aspect of the turbinates and the medial face of the bulb. (d) OMP-taulacZ mouse (Mombaerts et al., 1996). Olfactory marker protein (OMP) is expressed in all mature OSNs. The taulacZ marker was revealed as a blue precipitate by incubation with Xgal. OE, olfactory epithelium; OB, olfactory bulb; CP, cribriform plate, separating nasal from cranial cavity; RE, nonneuronal respiratory epithelium. The dorsoventral (D-V) orientation of the epithelium and the anteroposterior (A-P) alignment of the nasal cavity are indicated. This view reveals endoturbinates II, II′, III, and IV. *MOR23* targeted (e) and transgenic mice (f and g) express the taulacZ marker along with MOR23. In the medial hemisphere of the bulb, labeled axons converge invariably to a single target glomerulus. Individual transgenic lines show labeled cell densities that are either below (g) or above (f) the reference pattern (e). The MOR23-lacZ (e) and ES-Tg-I (g) mice are homozygous, and the TgSN-2 mouse (f) is hemizygous. Mice were 3–3.5 weeks old. In some cases, the images were flipped along a vertical axis to point in the same direction. Scale bars, 500 μm.

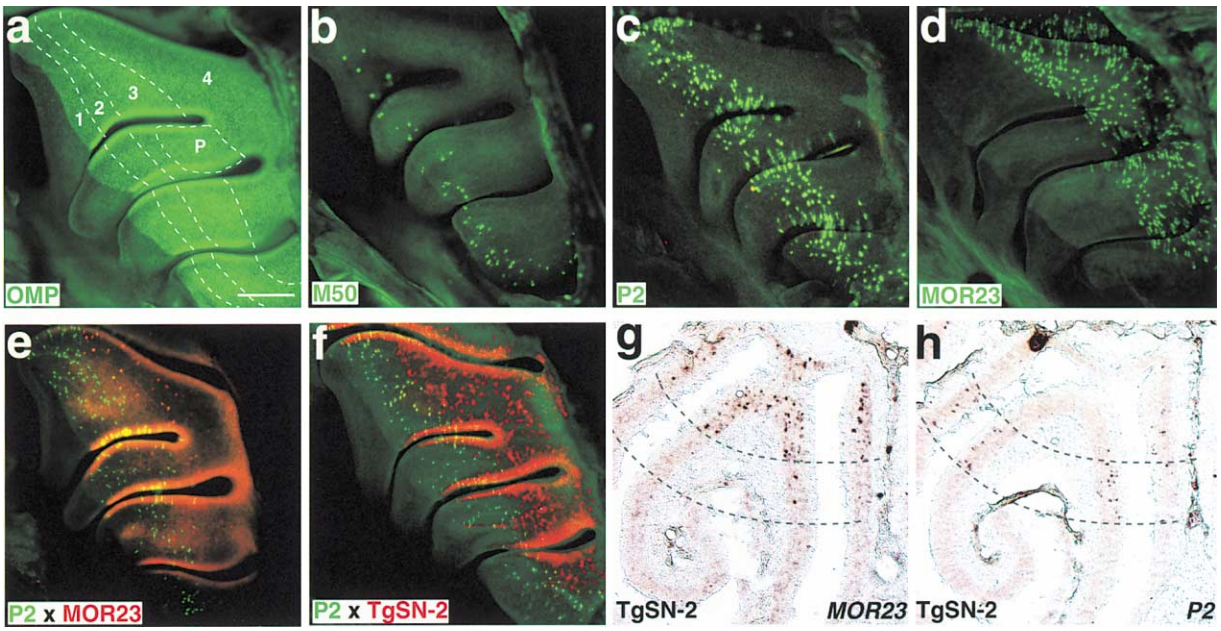

Figure 2. *MOR23* Targeted and Transgenic Expression in Zone 4 of the Olfactory Epithelium

Neuronal distribution of expression in the olfactory epithelium was assayed in whole-mount specimens. GFP was imaged by its intrinsic green fluorescence. β-galactosidase activity was revealed by exposure to Xgal and Fast Red Violet LB and imaging of the red fluorescence. (a–d) GFP-tagged targeted alleles of OMP or various OR genes illustrate the zonal boundaries. (a) OMP-GFP expression; four expression zones (1, 2, 3, 4) and a patch (P) (Strotmann et al., 2000; Pyrski et al., 2001) are shown diagrammatically. (b–d) Zone-specific expression of M50-GFP (zone 1) (P.F. et al., unpublished data); P2-GFP (zone 3); MOR23-GFP (zone 4). (e and f) β-galactosidase activity (red) reveals neurons expressing the targeted MOR23-lacZ (e) or the transgenic TgSN-2 (f) alleles. These cells define a zone dorsal to the zone of P2-GFP-expressing neurons and thus corresponding to zone 4. Note that a fine degree of intermingling between MOR23 and P2-expressing cells exists at the zone 3/4 boundary. TgSN2 is expressed in ~4-fold as many cells as the reference MOR23 targeted allele. Scale bar (a–f), 500 μm. (g and h) In situ RNA hybridization of serial coronal sections of a TgSN-2 heterozygous mouse using probes for *MOR23* (g) or *P2* (h). The cells expressing the *MOR23* endogenous gene or the TgSN-2 transgene define a zone that is dorsal to the cells expressing P2. Dorsal is to the top. All mice shown are heterozygous for the targeted alleles or hemizygous for the transgene, except (a) is a OMP-GFP homozygote, and (d) is a MOR23-GFP homozygote. Mice were P9 to P11 (a–f) or 3 weeks old (g and h).

of which exhibited β-galactosidase activity in OSNs, termed ES-Tg-I and ES-Tg-II (Table 1). For the *SN-IRES-GFP-IRES-taulacZ-neo* construct, all four mouse lines generated showed transgene expression in OSNs, although in some cases in only a few cells. We focused on the line with the highest number of labeled OSNs and consistent convergence to glomeruli: ES-Tg-III. None of the nonhomologous integrations in the three ES-Tg lines occurred near the *MOR23* or any other known OR locus (see Experimental Procedures).

In contrast to the ES-Tg strains, which were preselected at the level of ES clones, transgenic strains generated by pronuclear injection, termed TgSN, generally carry multiple copies of the transgene, some of which may be truncated or rearranged. We obtained two strains with at least one intact copy of the transgene, TgSN-1 and TgSN-2, both of which express the transgene in OSNs (Table 1).

Expression of the *MOR23* SN Transgene

In total, five lines carrying the MOR23 SN transgene show robust expression with consistent glomerular convergence (Table 1). Their expression patterns (Figures 1f and 1g) parallel those of MOR23-lacZ and MOR23-GFP. Labeling is restricted to mature OSNs, punctately distributed within zone 4 (compare zone distributions in Figures 2a–2e). This pattern is seen in all three ES-Tg lines and in TgSN-2. In TgSN-1, expression appears slightly shifted to overlap zones 4 and 3 in some animals. TgSN-2 mice were crossed to mice carrying the *P2-IRES-tauGFP* allele, expressed in zone 3 (P2-GFP, P.F. et al., unpublished data), and zonal distribution was examined in two-color whole-mounts (Figure 2f). TgSN-2-expressing OSNs are distributed dorsally to P2-expressing OSNs, thus in zone 4. This was confirmed by performing in situ RNA hybridization on serial coronal sections of TgSN-2 heads, using probes specific for the transgene (*lacZ*), *MOR23* and *M12* (zone 4), *P2* and *M50* (zone 1) (Figures 2g and 2h and data not shown). Axons of labeled OSNs converge invariably in each hemisphere onto a single glomerulus (Table 1). Glomerular convergence is a prediction from singular expression of the *MOR23* transgene, i.e., it suggests that transgene-expressing OSNs do not express other OR genes. We determined that these glomeruli correspond to the cognate MOR23 glomeruli in mice hemizygous for ES-Tg and heterozygous for MOR23-GFP. Axons of transgene-expressing OSNs (red) coconverge with OSNs expressing the endogenous *MOR23* gene (green) onto the same glomeruli, in which they intermingle diffusely (Figure 3h and Table 1).

The number of transgene-expressing OSNs deviates

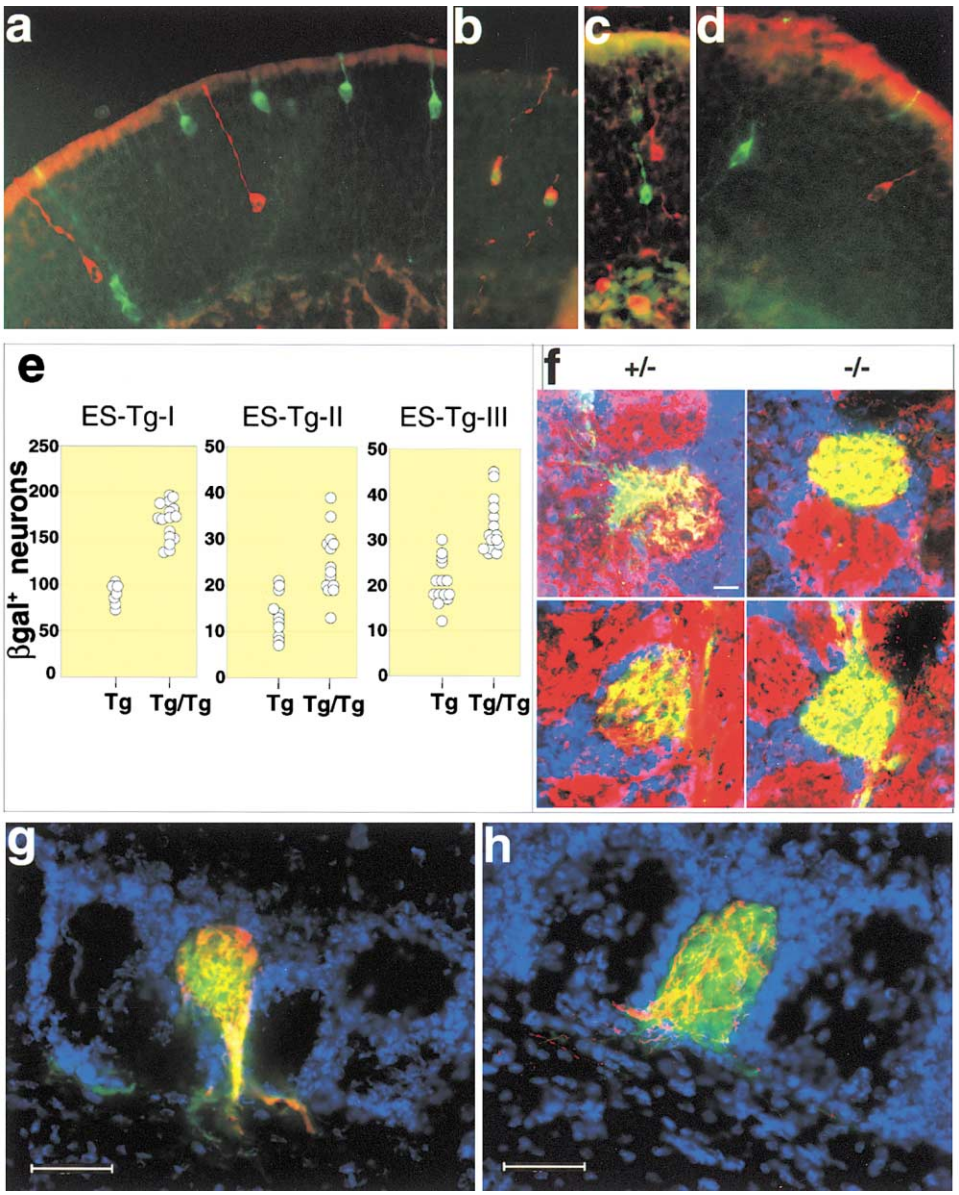

Figure 3. Monoallelic Expression of *MOR23*, Mutually Exclusive Expression of the *SN* Transgene, and Glomerular Coconvergence

(a) Olfactory epithelium of a MOR23-lacZ/MOR23-GFP mouse. Sections are stained with anti-β-galactosidase antibodies followed by Texas red-conjugated secondary antibodies. Individual neurons are either red or green fluorescent.

(b) Doubly labeled neurons are observed in a homozygous MOR23-GFP-lacZ mouse.

(c and d) The epithelium of a mouse hemizygous for ES-Tg-I and heterozygous for MOR23-GFP shows neurons that are either red or green fluorescent.

(e) The numbers of labeled cells in ES-Tg strains are twice as high in homozygous (Tg/Tg) versus hemizygous (Tg) mice. Numbers are plotted for half-heads, as proposed by Ebrahimi and Chess, 2000. The differences in distribution Tg versus Tg/Tg are statistically significant, with $p < 0.0001$ using Student's t test. The (Tg/Tg)/Tg ratio values are 1.88 (ES-Tg-I), 1.92 (ES-Tg-II), and 1.52 (ES-Tg-III). Note that the *y* axis values are different for ES-Tg-I.

(f) Sections of bulbs of MOR23-GFP mice stained with anti-NCAM antibody (red). Glomeruli of heterozygous mice (+/−, left panels) show an intermingling of red and yellow (red + green) axons, whereas glomeruli of homozygous mice (−/−, right panels) are fully doubly labeled (yellow). The red-only axons of the heterozygous glomeruli represent most likely axons expressing the wild-type, unmodified allele of *MOR23*. Periglomerular cells are identified with the nuclear stain TOTO-3 (blue). Scale bar, 20 μm.

(g) Bulb of a MOR23-lacZ/MOR23-GFP mouse. Red and green axons coinnervate the same glomerulus in the medial hemisphere.

(h) Bulb of a mouse hemizygous for ES-Tg-I and heterozygous for MOR23-GFP. Axon terminals of transgene-expressing OSNs (red) intermingle profusely with axons from OSNs expressing endogenous *MOR23* (green), forming a single glomerulus in the lateral hemisphere. Scale bar, 40 μm for (g) and (h).

Table 1. Quantification of Expression of the *MOR23* Transgenes

Transgenic Construct	Mouse Line	Tg Copy #	βgal$^+$ Neurons on Turbinate Epithelium		Olfactory Bulb Convergence Index		#Glom.	MOR23 Coconvergence
			Tg	Tg/Tg	Tg	Tg/Tg	Tg	Tg
SN-iTLneo	ES-Tg-I	1	90 ± 11 (7)	169 ± 20 (16)	100% (24)	100% (36)	1 (24)	33/33
(9.4 kb)	ES-Tg-II	1	13 ± 5 (11)	25 ± 7 (14)	86% (14)	97% (30)	0 (2);1 (12)	2/2[a]
SN-iG-iTLneo (9.4 kb)	ES-Tg-III	1	21 ± 5 (14)	32 ± 7 (14)	100% (16)	100% (22)	1 (16)	4/4[a]
TgSN	TgSN-1	1.5	18 ± 9 (8)	–	38% (8)	–	0(5); 1(3)	–
(9.4 kb)	TgSN-2	50–60	∼1500	–	100% (6)	–	1 (6)	2/2 (WM)
TgΔ	TgΔ-3	30–40	8 ± 3 (8)	–	63% (8)	–	0 (3); 1 (5)	–
(4.9 kb)	TgΔ-4	20–30	163 ± 47 (8)	–	100% (20)	–	1 (18); 2 (2)	–
	TgΔ-5	15–20	∼700 (18)	–	100% (18)	–	1 (18)	2/2
	TgΔ-6	1	0 (8); 1 (2)	–	0% (9)	–	0 (9)	NA
TgΔΔ	TgΔΔ-7	∼30	∼1500	–	100% (10)	–	3	30/30; 2/2 (WM)
(3.5 kb)	TgΔΔ-8	∼4	0 (24)	–	0% (24)	–	0	NA
	TgΔΔ-9	15–20	51 ± 14 (11)	–	100% (16)	–	1 (7); 2 (6); 3 (3)	4/4
Tg3′Δ[b]	Tg3′Δ-13	∼5	66 ± 41 (2)	–	100% (2)	–	3 (2)	–
(2.2 kb)	Tg3′Δ-19	∼3	157 ± 13 (2)	–	100% (10)	–	2 (10)	11/16
Tg5′Δ[c] (3.2 kb)	Tg5′Δ- 25 to 33		0 (4)[c]	–	0% (4)	–	0 (4)	NA
H.R.	**MOR23-lacZ**		**358 ± 19 (6)**					

Transgenic construct: the size of the *MOR23* sequences present in the construct is indicated between parentheses. βgal$^+$ neurons on turbinate epithelium: count of OSNs located on the medial face of endoturbinates II, II′, III, and IV in half-head whole-mount specimens. Shown is the average ± standard deviation, followed in parentheses by the total number of half-heads analyzed. When the count was >500, an estimate is given. For comparison, data are given for heterozygous MOR23-lacZ mice in bold on the last line of the table (H.R., homologous recombinant). Tg, mouse hemizygous for the transgene. Tg/Tg, mouse homozygous for the transgene. OB Convergence Index: percentage of bulbs showing convergence of fibers on a glomerulus-like structure on their medial face, as determined on Xgal-stained whole-mount specimens, followed in parentheses by the total number of bulbs analyzed. # Glom.: number of medial glomeruli observed per bulb, followed in parentheses by the number of bulbs displaying that number of glomeruli. This analysis was performed on whole-mount specimens of hemizygous mice. MOR23 Coconvergence: Coconvergence of the transgene-expressing axons with the axons of OSNs expressing the endogenous gene (MOR23-GFP) was assayed on immunostained tissue sections of mice heterozygous for MOR23-GFP and hemizygous for the transgene. Shown is the number of glomeruli displaying coinnervation, out of the total number of cognate MOR23 glomeruli analyzed. "WM" refers to this analysis done in whole-mounts. All analyses were performed with 3- to 4-week-old mice. –, not determined; NA, not applicable.

[a] Small number of βgal$^+$ axons.

[b] For transgenic construct Tg3′Δ, only the two most robustly expressing lines from the 14 we generated are listed. Another six transgene integration sites showed expression, albeit in few cells.

[c] For transgenic construct Tg5′Δ, nine independent genomic integration sites were analyzed. Eight of them showed no expression. One line exhibited an aberrant, exclusively ventral expression pattern in the epithelium.

from the reference pattern (Table 1). We counted Xgal-labeled cell bodies visible on the medial aspect of turbinates II, II′, III, and IV in whole-mount specimens (Ebrahimi and Chess, 2000). The lines with a single copy of the transgene express fewer labeled cells than the reference MOR23-lacZ mice, but lines with a high copy number can exhibit up to 4-fold the reference cell density. There is no strict correlation, however, between transgene copy number and number of transgene-expressing cells.

In a given transgenic line, the number of transgene-expressing OSNs is increased 2-fold in homozygous compared to hemizygous mice (Figure 3e and Table 1). The staining intensity of the cells is similar. Thus, OSNs of homozygous mice are twice as likely to choose the transgene for expression, suggesting that each allele of the transgene in a homozygous animal has an independent probability to be expressed. This is consistent with the transgene being monoallelically expressed in homozygous mice, like its endogenous counterpart and other OR genes (Ebrahimi et al., 2000).

Dual analysis of marker expression in ES-Tg or TgSN mice crossed to MOR23-GFP mice indicates that the transgene and the endogenous gene are expressed in mutually exclusive subsets of OSNs: cells are either red or green fluorescent (Figures 3c and 3d) (Serizawa et al., 2000).

M71 Transgenic Mice

We extended our findings to another OR gene, *M71*. Mice were generated carrying either a targeted *M71-IRES-taulacZ* (M71-lacZ strain) or *M71-IRES-tauGFP* (M71-GFP strain) allele (Figure 4a). Intercrossing indicates that the *M71* gene is also subject to monoallelic expression (data not shown). We assembled an *M71-IRES-taulacZ* transgene that is identical to the targeting vector but lacking the *neo*-selectable marker. Transgene M71-Tg contains 9.2 kb of genomic sequence, with 2.3

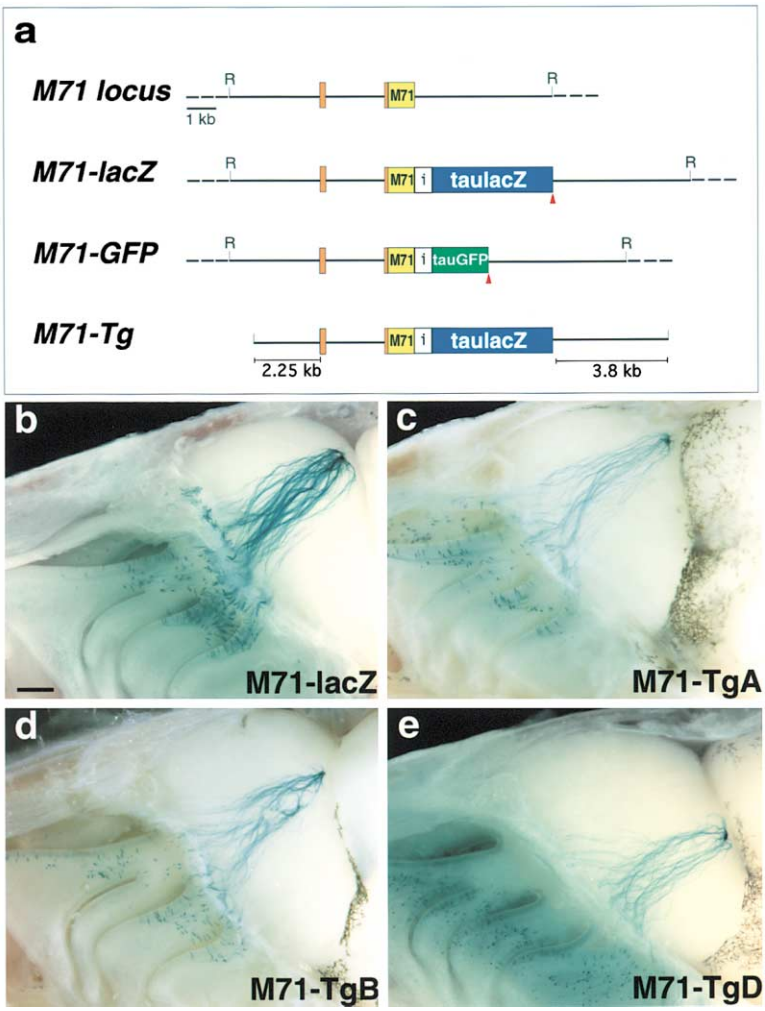

Figure 4. *M71* Transgenic Mice

(a) Structure, targeted mutagenesis, and transgenesis of *M71*. (*M71 locus*) The coding sequence (yellow box) and 5′ noncoding sequences (orange boxes) are shown. 5′RACE analysis mapped a putative TSS 2.2 kb upstream of the ATG. The 5′ noncoding exon is 175 bp and is followed by a 2.0 kb intron that ends 18 bp upstream of the start codon. R, EcoRI. (*M71-lacZ*) The targeted *M71-IRES-taulacZ* allele after Cre-mediated recombination. (*M71-GFP*) The targeted *M71-IRES-tauGFP* allele after Cre-mediated recombination. (*M71-Tg*) The transgene.

(b–e) Whole-mount specimens of a M71-lacZ heterozygous mouse (b) and hemizygous mice of various transgenic lines (c–e). In line M71-TgD (e), most of the labeled OSN cell bodies show a ventral shift compared to the reference pattern (b). Note that this correlates with a ventral shift of the medial glomerulus in the bulb. Mice were 3–4 weeks old. Scale bar, 500 μm.

kb upstream of the putative TSS and 3.8 kb downstream of the coding region (Figure 4a). Ten transgenic lines were generated by pronuclear injection. Seven of them showed expression in OSNs of Xgal-stained whole-mount specimens, but in three lines, the number of cells was low and the pattern uninterpretable. The four lines with the highest numbers of cells were examined further. Restriction to zone 4 was seen in three of them (M71-TgA, B, and C) (Figures 4c and 4d). For M71-TgB, serial coronal sections of the epithelium were either exposed to Xgal or processed for in situ RNA hybridization using probes for *M12*, an OR gene expressed in zone 4; we thus confirmed restriction of expression to zone 4 (data not shown). In the fourth line (M71-TgD), zonal restriction is lost, with most labeled cells in zone 3 and a few residing in the appropriate zone (Figure 4e and data not shown). In this line, one of the three transgenic copies is truncated at the 3′ end.

A single labeled glomerulus on average was observed in the medial and lateral hemispheres of each bulb in all four lines. In M71-TgA, B, and C, the labeled glomeruli are in a region of the bulb comprising the cognate M71 glomeruli. In M71-TgD, the labeled glomeruli are ventral to the M71 glomeruli in both hemispheres (Figure 4e and data not shown). The ventral shift of epithelial zone of expression exhibited by this line is thus accompanied by a ventral shift of the labeled glomeruli. To show conclusively that the labeled axons converge to the M71 glomeruli, we analyzed sections of mice hemizygous for M71-TgA or B and heterozygous for M71-GFP: we found a perfect concordance of green (endogenous M71) and red (transgenic M71) glomeruli in all bulbs (data not shown). In M71-TgD mice, most transgene-expressing neurons converge to ectopic red glomeruli, but a minority of them innervate the cognate green glomeruli (see below, Figure 8e). In the epithelium, we verified mutually exclusive expression of the transgene and the endogenous gene (data not shown). These crosses also provided genetic evidence that the transgenes are unlinked to the endogenous locus.

Deletion of Intronic Sequences

We have thus defined for two OR genes ∼9 kb DNA segments that function autonomously. These transgenes are chosen for expression by a population of OSNs, which send axons to the cognate glomeruli. To map the sequences that confer this competence and to attempt to uncouple these regulations, a deletion series was generated for the 9.4 kb (SN) *MOR23* transgene.

OR genes contain typically one or a few introns in

their 5′ noncoding region, suggesting that they may contribute regulatory sequences. To test the role of the introns in OR gene regulation and to determine if splicing is required for OR gene expression, we assembled two *MOR23* deletion constructs, designated TgΔ and TgΔΔ, in which intron 2 (4.5 kb) and both introns 1 and 2 (a total of 5.9 kb), respectively, are precisely excised (Figure 5a). We generated by pronuclear injection four lines with the TgΔ construct (TgΔ-3 to TgΔ-6; Table 1) and three lines with the TgΔΔ construct (TgΔΔ-7 to TgΔΔ-9; Table 1).

The expression pattern of the TgΔ lines is similar to the reference MOR23 pattern. We focused primarily on the line with the highest number of transgene-expressing OSNs, TgΔ-5 (Figures 5d and 5e). In crosses with P2-GFP mice, transgene expression was exclusive of the P2 zone and restricted to zone 4 (Figure 5e). Axons project invariably to the cognate MOR23 glomeruli (Table 1). In some TgΔ-4 mice, the expression in zone 4 extends slightly ventrally into endoturbinate II′, which corresponds to the "P" area shown in Figure 2a. Interestingly, some transgene copies are truncated in TgΔ-4, while this is not the case in TgΔ-5, which exhibits correct zonal restriction.

In TgΔΔ-7 and -9 lines, restriction of expression to the dorsal zone appears to be lost. TgΔΔ-7 is expressed in OSNs distributed throughout zones 4, 3, and 2. The pattern is nonuniform, generally displaying a conspicuous middle band of highest cell density (Figure 5f). By crossing TgΔΔ-7 mice with P2-GFP mice, we defined the domain of maximal density of transgene-expressing OSNs as the ventral part of zone 4 together with zone 3 (Figure 5g). Correlated with this extended epithelial pattern, an extended pattern of axonal projections to the bulb is observed (see below, Figures 7a and 7b): in addition to the single labeled glomerulus located centrally in the medial hemisphere, as in MOR23-lacZ, TgSN or TgΔ mice, two sequentially more ventral glomeruli are present in all TgΔΔ-7 bulbs (Table 1). A similar pattern of ectopic glomeruli is observed in more than half of TgΔΔ-9 bulbs (Figure 7b and Table 1). These glomeruli are aligned along a dorsoventral axis, defining a dorsal, middle, and ventral glomerulus. A possible interpretation of this arrangement is that the three glomeruli represent discrete convergence loci from OSNs whose cell bodies reside in different epithelial zones.

A 395 bp Upstream Region Is Required for *MOR23* Transgene Expression

The TgΔΔ construct is expressed robustly in OSNs while consisting only of 0.4 kb 5′ of the putative TSS, a 1.4 kb fusion of the three exons and 1.7 kb 3′ of the stop codon. We next generated truncations in either 3′ or 5′ of the cDNA core to assemble constructs Tg3′Δ and Tg5′Δ, respectively (Figure 5a).

In Tg3′Δ, the 3′ end of the TgΔΔ construct is truncated by 1.4 kb, preserving ∼300 bp 3′ of the stop codon. The 300 bp region contains the unique polyadenylation signal of the 1.7 kb 3′ region. This truncation did not abolish or grossly alter expression of the transgene (Figure 5i and Table 1). Punctate OSN-specific expression was seen in five of eight transgenic founder animals and in three of six independent transgenic lines. Of these 14 transgene integrations, three showed robust expression. *LacZ*-expressing OSNs are distributed mostly but not exclusively in zone 4, and their projections converge medially onto one to three glomeruli (Figure 5i). The dorsal-most glomerulus is the MOR23 cognate glomerulus, as shown in mice expressing MOR23-GFP and Tg3′Δ-19 (Table 1). To our knowledge, Tg3′Δ is the smallest construct (2.2 kb of spliced genomic sequence including the 0.9 kb coding region) reported to confer basic properties of OR gene expression: OSN-specific, punctate expression and coconvergence to cognate glomeruli.

To build Tg5′Δ, a region of 395 bp 5′ of the TSS was deleted from TgΔΔ, up to position −10. Three transgenic founders showed no *lacZ* expression in either epithelium or bulb at 4 weeks of age. Transgenic offspring of six additional founders lacked expression in five of six lines (Figure 5j and Table 1). In one line, labeled OSN cell bodies were observed, located exclusively in zone 1 (data not shown). Because this pattern is seen only in 1/9 integration sites of Tg5′Δ, we hypothesize that it results from the occasional dominant effect of flanking DNA sequences (Pyrski et al., 2001). This also suggests that we have not deleted all sequences involved in OR expression in Tg5′Δ.

Putative O/E and Homeodomain Binding Sites

Our transgenic results offer an opportunity to restrict OR sequence analysis to short experimentally defined control regions. The smallest expressing *MOR23* transgene (Tg3′Δ) contains 405 bp 5′ of the TSS and 503 bp of 5′ noncoding exons. The 405 bp upstream region consists of a *LINE-1* fragment followed by only 148 bp of unique sequence. The analogous region in the smallest expressing *M71* transgene has 161 bp upstream of the TSS (data not shown), followed by the 175 bp noncoding exon. Analysis of these regions and putative control regions of other OR genes (Figure 6) using Consensus and Gibbs Sampler algorithms on both DNA strands (see Experimental Procedures) yielded an O/E (olf-1)-like site (Wang et al., 1997) with consensus *MTCCCAG GAGVH*. All sites contributing to this consensus contain a core Y_3CAR_4, in which at least one of the pyrimidines is *C* and at least one purine is *G*. There are six occurrences of this core motif in *MOR23*, one in *M71*, three in *M72*, and at least two in *OR37A*, *B*, *C*, *D*, and *E* each, all found in close proximity (−250 to +150) of the TSS. The zebrafish *OR2.1* gene, which is the only OR gene from another species for which transgenic expression has been achieved (Mori et al., 2000), also shows this motif. The *OR2.1* homology contributes to a previously identified 13-mer motif *CTCTCAAGAGATG*, found upstream of many zebrafish OR genes (Dugas and Ngai, 2001). This analysis also revealed that the Tg5′Δ construct, expressed in 1/9 lines, retains two of six O/E-like sites.

Furthermore, we identified a conserved *TAATTG* sequence at approximately −100 of various OR genes (Figure 6), reminiscent of a homeodomain binding site (Mann, 1995). Remarkably, the spacing between this putative homeodomain binding site and the O/E-like site is conserved in many OR genes (Figure 6).

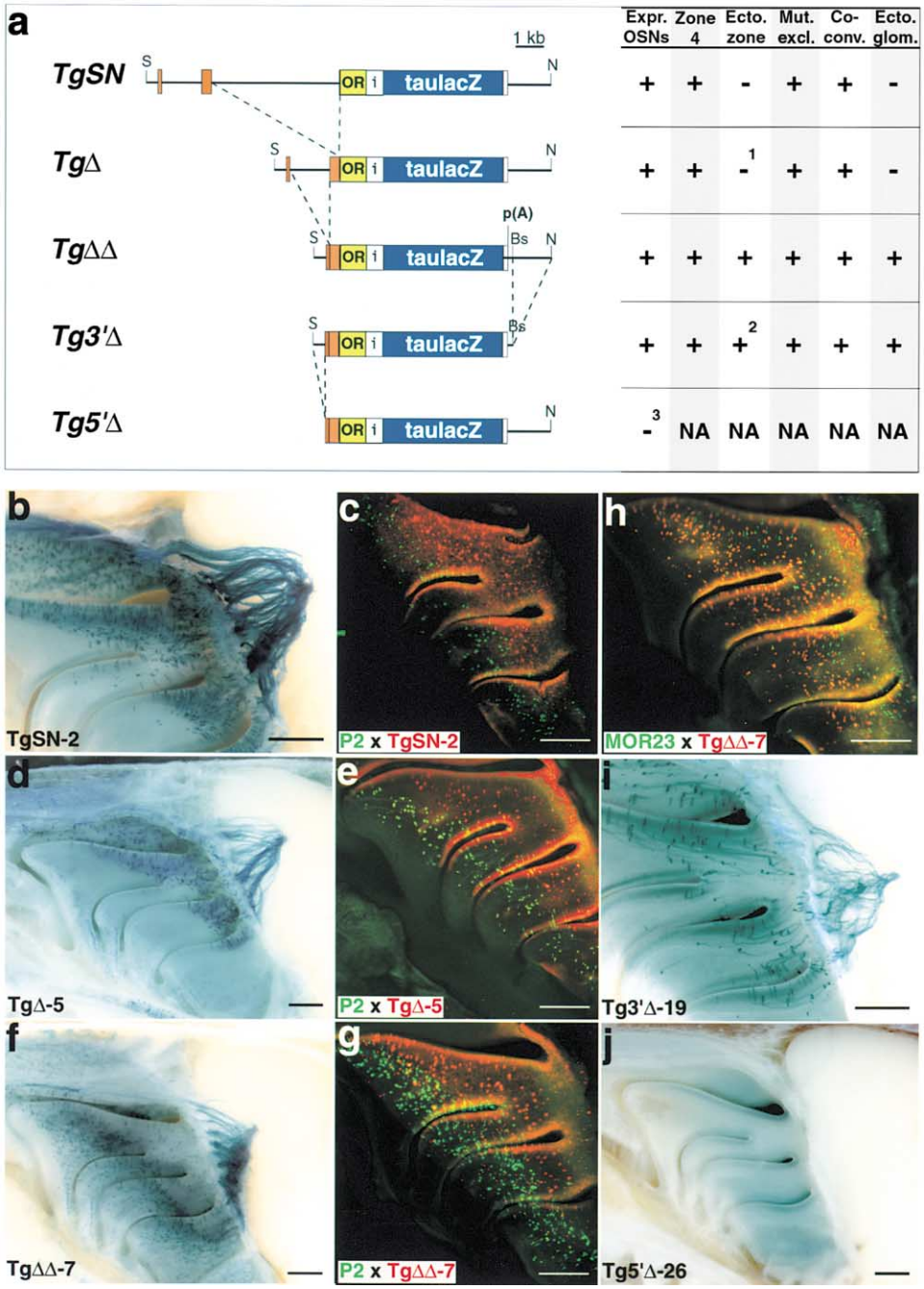

	Expr. OSNs	Zone 4	Ecto. zone	Mut. excl.	Co-conv.	Ecto. glom.
TgSN	+	+	-	+	+	-
Tg∆	+	+	-[1]	+	+	-
Tg∆∆	+	+	+	+	+	+
Tg3'∆	+	+	+[2]	+	+	+
Tg5'∆	-[3]	NA	NA	NA	NA	NA

Figure 5. Deletion Series of the *MOR23* Transgene

(a) (Left) Transgenic constructs. TgSN is the original 9.4 kb Sac-NheI genomic fragment tagged with *IRES-taulacZ*. A deletion of intron 2 (4.5 kb) results in Tg∆, and an additional deletion of intron 1 (1.4 kb) results in Tg∆∆. The latter construct was further truncated at the 3′ end by 1.4 kb, resulting in Tg3′∆, or at the 5′ end by 0.4 kb, resulting in Tg5′∆. (Right) Properties of the transgenic expression patterns are summarized. Expr. OSNs, expression in OSNs. Zone 4, expression in zone 4. Ecto. zone, expression outside zone 4. Mut. excl., transgene expression is mutually exclusive with the expression of the endogenous *MOR23* gene. Co-conv., glomerular coconvergence of axons from transgene-expressing OSNs with axons from OSNs expressing the endogenous counterpart. Ecto. glom., ectopic glomeruli. [1]The Tg∆-5 line is restricted to zone 4, but Tg∆-4 is expressed in zone 4 with a slight ventral extension of expression. [2]A minority of labeled cells are observed outside zone 4. [3]One of nine transgenic lines displays labeled cells in the ventral-most zone, zone 1.

(b–h) Whole-mount specimens of half-heads of hemizygous transgenic mice, stained with Xgal alone (b, d, f, i, and j) or Xgal in presence of Fast Red Violet LB (c, e, g, and h). The number of the individual transgenic line follows the hyphen (Table 1). Epithelial expression and glomerular convergence are detected with all constructs except Tg5′∆ (j). Neuronal distribution can be assessed in the epithelium of mice hemizygous for the transgene and heterozygous for P2-GFP (c, e, and g) or for MOR23-GFP (h). TgSN-2 (c) and Tg∆-5 (e) are expressed in a zone dorsal to the zone where P2-GFP is expressed, whereas Tg∆∆-7 (g and h) is expressed throughout zones 4, 3, and 2. Mice were 3–4 weeks old (b, d, f, i, and j) or P10 (c, e, g, and h). Scale bars, 500 μm.

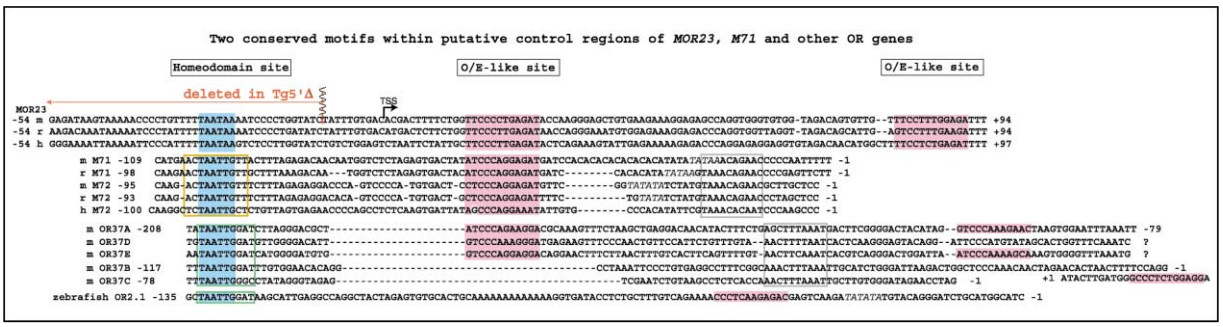

Figure 6. Sequence Analysis of OR Gene Putative Control Regions

Inter- and intraspecies comparison of upstream regions of 13 mammalian OR genes and the zebrafish *OR 2.1* gene (Dugas and Ngai, 2001) reveals two conserved motifs: homeodomain binding sites (blue boxes) and O/E-like sites (pink boxes). A third conserved motif for M71/M72 genes lies close to the TSS (gray box). Further homologies encompassing the homeodomain sites could be observed for mouse, rat, and human *M71* and *M72* genes (orange box) and for *OR37A-E* and *OR2.1* (green boxes). Potential *TATA* box sequences are in italics. *OR37A-E* green and gray boxes were identified previously as motif block I and IV, respectively (Hoppe et al., 2000). The wavy line in the *MOR23* sequence indicates the breakpoint of the deletion in Tg5′Δ. TSS indicates *MOR23* upstream-most nucleotide found in 5′RACE products from olfactory mucosa RNA.

Rerouting to Ectopic Glomeruli

To further characterize the innervation patterns of the multiple MOR23 glomeruli of TgΔΔ-7 mice, we examined coronal sections through the bulbs of mice hemizygous for the transgene and heterozygous for MOR23-GFP. Glomeruli are distributed along two virtual curves, one on the medial surface and the second shifted anteriorly and dorsally, on the lateral surface of the bulb. There are three glomeruli on the medial face (M1, M2, and M3, from dorsal to ventral) and four glomeruli on the lateral face (L4, L3, L2, and L1, from ventral to dorsal). The dorsal-most glomeruli (M1 and L1) are heavily innervated by MOR23-GFP axons and correspond to the cognate MOR23 glomeruli; as expected, they are coinnervated by axons of transgene-expressing OSNs (Figures 7c–7e). The next, more ventral ectopic glomeruli (M2 and L2, L3) are predominantly formed by axons of transgene-expressing OSNs, but, surprisingly, they are coinnervated by a significant number of axons from OSNs expressing the endogenous *MOR23* gene (Figures 7f–7h). This observation was made for the medial glomeruli of 13/14 bulbs and for the lateral glomeruli of 15/15 bulbs. It was specific for axons expressing the endogenous *MOR23* gene, as axons expressing either the *P2*- or *M72-IRES-tauGFP* alleles do not coinnervate the TgΔΔ-7 ectopic glomeruli (data not shown). Note that MOR23-M2 ectopic glomeruli and P2 medial glomeruli are located in very close proximity to each other (in some cases a single glomerulus apart, data not shown). Thus, these data suggest that overall axonal trajectories are not impaired in the TgΔΔ-7 line but that the transgene leads to specific mistargeting of MOR23-expressing axons. The next, ventral-most ectopic glomeruli found at the level of the ventral floor of the bulb (M3 and L4) can also be innervated by MOR23-GFP axons, but this is a rarer event than for the M2, L2, and L3 ectopic glomeruli: 3/8 M3 glomeruli (Figures 7i–7k) and 1/9 L4 glomeruli were coinnervated by MOR23-GFP axons (24% overall frequency). Based on their innervation patterns, the M1 and L1, the M2 and L2/ L3, the M3 and L4 glomeruli are equivalent and likely represent the two mirror-image glomerular maps of the bulb (Nagao et al., 2000).

The innervation of ectopic glomeruli by MOR23-GFP neurons is not accompanied by a major alteration of the zonal distribution of their cell bodies into more ventral zones (Figure 5h). A small minority of cells residing outside zone 4 is always observed. Subtle changes involving less than 10% of cells, particularly at the boundary between zones 3 and 4, where MOR23 and P2-expressing neurons are known to intermingle, are however difficult to document and cannot be ruled out.

To identify the zonal origins of axons forming the glomeruli of TgΔΔ-7 mice, sections were immunostained for the olfactory cell adhesion molecule (OCAM) (Yoshihara et al., 1997). OCAM is expressed by axons of OSNs whose cell bodies reside within zones 1, 2, and 3, not 4. TgΔΔ-7-expressing neurons are distributed in zones 2, 3, and 4 and are thus expected to contain OCAM-positive and -negative populations. Serial sectioning of the bulbs of five TgΔΔ-7 hemizygous, MOR23-GFP heterozygous mice revealed that 20/20 dorsal-most glomeruli (M1 and L1) were overall OCAM negative (and located in the OCAM-negative region of the bulb), whereas 42/42 ectopic glomeruli (M2, M3, L2, L3, and L4) were overall OCAM positive (and located in the OCAM-positive region of the bulb) (Figures 7l–7p). This suggests that the dorsal-most glomeruli predominantly receive input from OSNs of zone 4, whereas the more ventral, ectopic glomeruli are predominantly innervated by OSNs from zones 3 and 2, consistent with a zone-to-zone projection pattern between olfactory epithelium and bulb. It is however difficult to assess the individual OCAM antigenicity of subsets of axons within glomeruli. Some of the axons of transgene-expressing OSNs innervating the dorsal-most glomeruli appeared OCAM positive, suggesting that they originate from zones 3 and 2. Conversely, some of the MOR23-GFP axons within ectopic glomeruli appeared OCAM negative, suggesting that they originate from OSNs in zone 4.

The recruitment of endogenous MOR23 axons into TgΔΔ-7 ectopic glomeruli suggests an active role of the OR in axon guidance and a significant degree of plasticity in bulb architecture (Strotmann et al., 2000). If this phenomenon is driven by interactions between

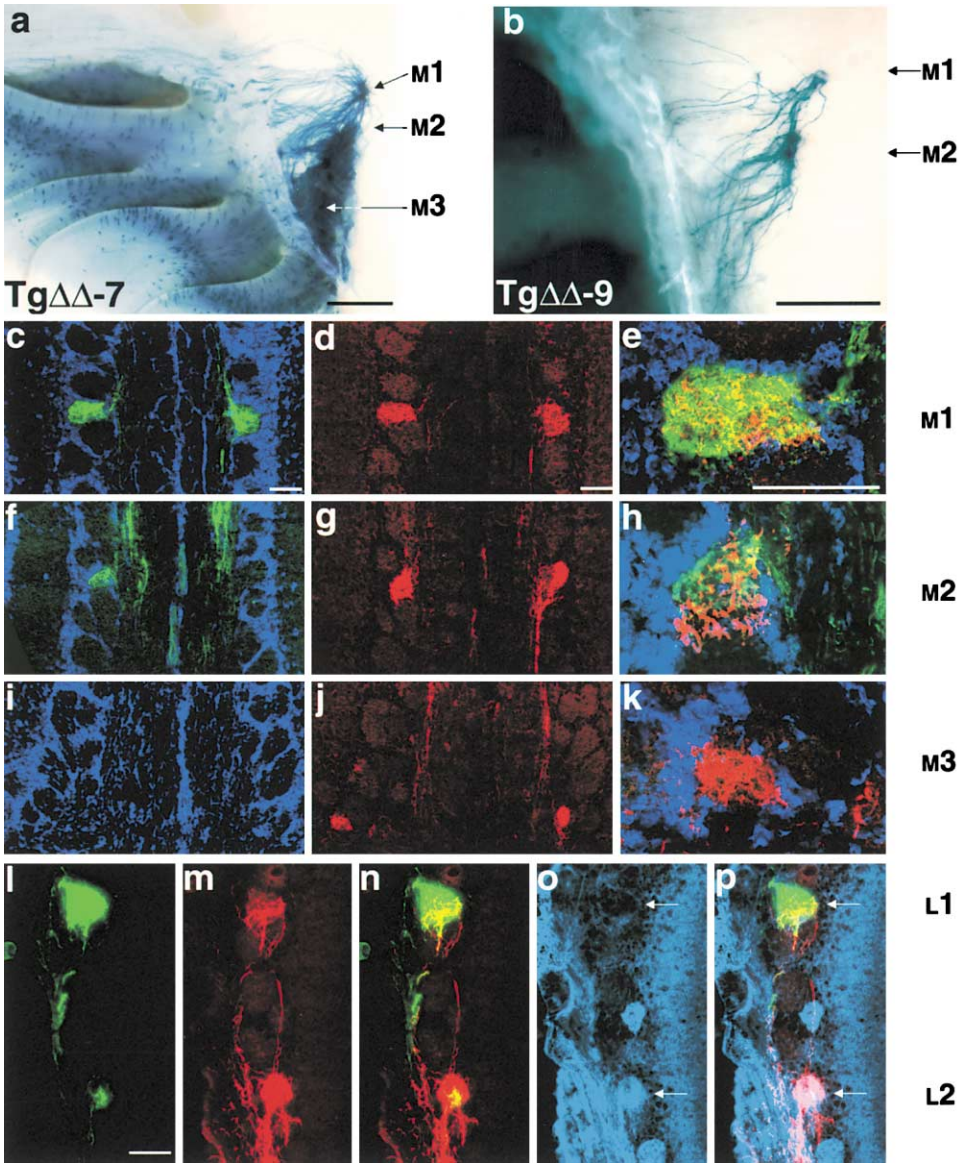

Figure 7. Axons of Endogenous and Transgenic *MOR23*-Expressing OSNs Coconverge to Cognate and Ectopic Glomeruli

(a and b) Medial views of Xgal-stained whole-mounts of TgΔΔ-7 (a) and TgΔΔ-9 (b) mice reveal ectopic, more ventral glomeruli (M2, M3) in addition to the cognate (M1) glomerulus. In TgΔΔ-7, a dense drape of labeled axons typically covers the M2 and M3 glomeruli. (c–k) Confocal microscope images of coronal sections through the bulbs of a 3-week-old mouse hemizygous for TgΔΔ-7 and heterozygous for MOR23-GFP. OSNs expressing the endogenous *MOR23* gene (green) and TgΔΔ-expressing OSNs (red) coinnervate the same glomeruli in the medial hemisphere of the bulbs. (c, f, and i) Green fluorescence with TOTO-3 nuclear counterstain (blue); (d, g, and j) red fluorescence. Dorsal is to the top. (c and d) The dorsal-most M1 glomeruli are innervated by both axonal populations. (f and g) A different section shows the pair of M2 ectopic glomeruli. A significant fraction of axons from OSNs expressing the endogenous *MOR23* gene innervates the left M2 glomerulus. (i and j) The ventral-most pair of M3 glomeruli shows innervation exclusively by axons of transgene-expressing OSNs. (e, h, and k) Higher magnifications of left glomeruli of the M1, M2, and M3 pairs, respectively. (l–p) The lateral hemisphere of a bulb of a 3-week-old mouse hemizygous for TgΔΔ-7 and heterozygous for MOR23-GFP reveals the dorsal-most L1 (cognate) and the L2 glomeruli on the same section. Both glomeruli are coinnervated by green (MOR23-GFP) and red (TgΔΔ-expressing) axons. Immunostaining for OCAM (turquoise blue, [o and p]) shows that the L1 glomerulus resides in the OCAM-negative region of the bulb, whereas the L2 glomerulus is OCAM-positive. This suggests that the bulk of the axons forming the L1 and L2 glomeruli originate from zone 4 and zones 3–2, respectively. Scale bars, 500 μm (a and b), 100 μm (c–p).

OSNs expressing the same OR, ectopic glomeruli formed by neurons expressing a different OR transgene should selectively recruit the axons of OSNs that express the cognate endogenous gene. In the M71-TgD strain, some transgene-expressing cells are correctly placed in zone 4, but a majority of them are mislocated in zone 3, and the glomeruli are shifted ventrally relative to the M71 cognate glomeruli. We found that these ectopic glomeruli recruit M71-GFP-expressing axons in 9/19 cases (Figures 8c, 8c′, and 8f). Reciprocally, a minor

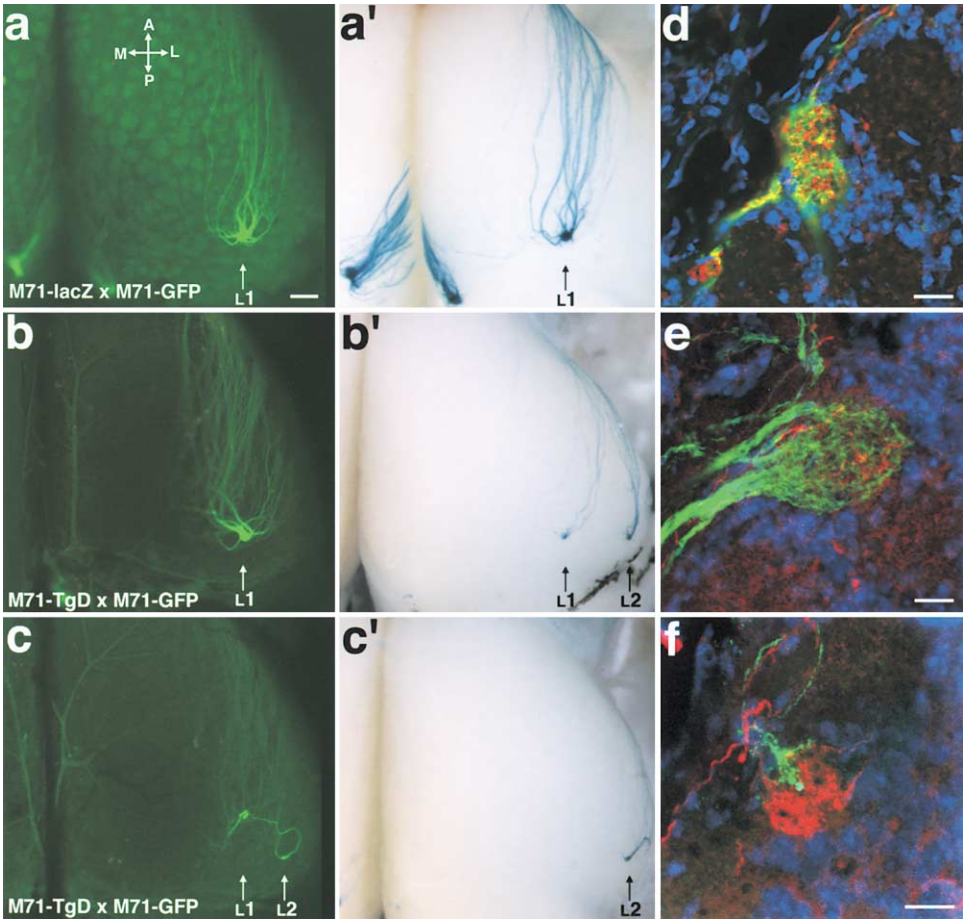

Figure 8. Coconvergence of Axons of M71-Expressing OSNs to Cognate and Ectopic Glomeruli

(a–c′) Dorsal view of individual bulbs imaged with fluorescent light (left panels) and subsequently stained with Xgal (middle panels). A, anterior; L, lateral; M, medial; P, posterior. (a and a′) A M71-lacZ/M71-GFP mouse showing lacZ-positive and GFP-positive axons coconverging to the M71 cognate glomerulus (L1) on the lateral side of the bulb. (b, b′, c, and c′) Two mice hemizygous for M71-TgD and homozygous (b and b′) or heterozygous (c and c′) for M71-GFP. The mouse in (b) and (b′) shows axons of TgD-expressing OSNs innervating both the cognate glomerulus (L1) and an ectopic L2 glomerulus, located laterally to L1. The mouse in (c) and (c′) shows axons of TgD-expressing OSNs innervating an ectopic L2 glomerulus (c′), which also receives input from M71-GFP axons (c). (d) Coronal sections through a M71-lacZ/M71-GFP bulb showing coconvergence and intermingling of the two axonal populations in a medial glomerulus. (e and f) Bulbs of mice hemizygous for M71-TgD and homozygous for M71-GFP. (e) Shows an M71 cognate medial glomerulus coinnervated by axons of TgD-expressing OSNs. (f) Shows an ectopic lateral glomerulus formed by axons of TgD-expressing OSNs and coinnervated by M71-GFP axons. Mice were 3 weeks old. Scale bars, 200 μm for (a)–(c′); 20 μm for (d)–(f).

population of axons from transgene-expressing cells innervates the cognate M71 glomeruli (Figures 8b, 8b′, and 8e).

Discussion

Compact and Proximal Control Regions

We demonstrate for two mouse OR genes that ~9 kb transgenes reproduce closely the expression properties of the endogenous counterparts in 7/9 transgenic lines. For *MOR23*, a minigene of 4.9 kb (TgΔ) can recapitulate the same features. Transplanted outside their resident gene cluster, these relatively short segments of genomic DNA function autonomously. Transgene-expressing OSNs do not simply read a cell-type specificity, as they do not coexpress the endogenous OR gene; instead, they define a novel cell population. The transgene-expressing OSNs are phenotypically identical to OSNs expressing the endogenous OR gene in many aspects, including one decisive criterion: their axons innervate the same glomeruli. Glomerular coconvergence is a sensitive readout of OR gene regulation and has not been shown previously for OR transgenes. It also suggests that transgene-expressing OSNs do not coexpress other OR genes and therefore that the transgenes, like endogenous OR genes, have the property of monogenic expression. Conversely, as endogenous MOR23-expressing cells do not coexpress the transgene, the transgenes have retained the ability to be silent in cells expressing other OR genes.

The smallest transgene allowing *MOR23* expression, Tg3′Δ, contains only 2.2 kb of spliced genomic sequence and includes a 395 bp upstream region shown to be required for transgene expression. Thus, OR gene choice and expression can be mediated by compact and proximal control regions, contrary to a prevailing

view of long-range control (Ebrahimi et al., 2000; Serizawa et al., 2000). Furthermore, expression in OSNs of intronless *MOR23* transgenes suggests that the 5′ introns, typically observed in OR genes, contain no essential sequence information and that splicing per se is not required for OR gene choice and expression.

Could the transgenes make use of unlinked DNA sequences for expression? DNA rearrangements in OSNs could juxtapose the transgenes to the true regulatory regions; *trans*-splicing would invoke unlinked promoters and exons. We have no evidence for either possibility from 5′ RACE data. However, genomic rearrangements affecting the nontranscribed part of OR loci remain a possibility.

The compactness of both coding and regulatory regions of OR genes may have facilitated the extraordinary amplification of the mammalian OR repertoire (Zhang and Firestein, 2002). The unit of OR gene evolutionary duplication and divergence may be <10 kb.

Long-Range Control?

Transgenic experiments with the OR gene *M4* suggested that a combination of short- and long-range controls regulate OR gene expression (Qasba and Reed, 1998). Using a non-OR-coding transgene consisting of a 6.7 kb upstream genomic fragment driving lacZ expression, two lines expressing the *M4* transgene were obtained, one restricted to the correct zone but the other to an ectopic zone. Our data do not argue for long-range control of zonal specification. TgΔ (4.9 kb) is expressed in the correct zone, whereas both Tg$\Delta\Delta$-7 and -9 (3.5 kb) have lost zonal restriction, suggesting that *MOR23* zonal expression is regulated proximally. Zonal patterning may however be particularly sensitive to the genomic context of transgene integration.

Transgenic expression of two other OR genes, *M12* (Ebrahimi and Chess, 2000; Ebrahimi et al., 2000) and *MOR28* (Serizawa et al., 2000; Ishii et al., 2001), was achieved by using YAC fragments of 300 kb and 200 kb, respectively. In apparent contrast with our findings, truncation of the *MOR28* YAC from 200 kb to 180 kb or 90 kb no longer afforded expression. We speculate that smaller *MOR28* transgenes (10 kb or less), had they been tried, might allow expression. The *MOR28* gene resides within the T cell receptor α gene cluster, another locus with complex regulation. Axons from *MOR28* transgene-expressing OSNs do not coconverge to glomeruli with those expressing the endogenous *MOR28* gene, in contrast to our observations for both the *MOR23* and *M71* genes. The reasons for this lack of coconvergence are unclear, making it difficult to ascertain whether regulation of the *MOR28* gene has been reproduced.

In an unusual finding, a minipromoter of the *OMP* gene, which is normally expressed in all mature OSNs, conveyed a punctate, OSN-specific expression pattern to a marker in a transgenic line in which the transgene integrated near an OR gene (Pyrski et al., 2001). This suggests that endogenous OR control regions have the potential to act on other promoters at longer distances. Likewise, we suggest that the single expressing Tg5′Δ line (lacking 395 bp of upstream sequence) among nine we obtained may result from an integration of the transgene in the vicinity of an OR gene, expressed in this case in zone 1. It is noteworthy that the OMP minimal promoter used in the above study contains an O/E-1 site, and similarly, Tg5′Δ retains two of the six O/E-like sites we identified in *MOR23* control regions. Proximal O/E sites may be able to interact with more distant regulatory elements.

OR Gene Control and Conserved Motifs

OR gene regulation can be conceptually dissected into multiple functions: expression is OSN specific, punctate (in nonadjacent cells), zonally restricted, singular (one allele of one OR gene per neuron), and associated with axonal projection to specific glomeruli. The ~9 kb transgenes for *MOR23* and *M71* are able to reproduce those features, with the single exception that the number of expressing OSNs varies from the reference targeted strain.

MOR23 minigenes Tg$\Delta\Delta$ (3.5 kb) and Tg3′Δ (2.2 kb) maintain these basic properties, with the exception that they may have lost zonal specificity of expression, suggesting loss of specific aspects of regulation. Further deletion of a 395 bp region 5′ of the putative TSS however abolishes expression. As the 5′ part of this region is a repetitive element, the necessary sequences may be confined within a segment as short as ~150 bp. Further supporting the importance of this segment is the presence of conserved motifs overlapping with it.

Based on our transgenic data and interspecies sequence alignments, the control regions of both *MOR23* and *M71* are likely to be extremely compact. For *MOR23*, alignment of mouse, rat, and human sequences terminates upstream of −150, suggesting an upstream boundary to the control region. For *M71* and its paralog *M72*, the interspecies alignment cannot be extended upstream of −250, and the strongest homologies lie within a ~160 bp region, consistent with transgenic data supporting the sufficiency of this region for expression (data not shown). Within the *M71/M72* upstream region, we identified three common elements, including a homeodomain binding site and an O/E-like site. Similar O/E-like sites have been noted previously upstream of the putative TSS in human OR genes (Sosinsky et al., 2000). The presence of S8 homeodomain binding sites has been suggested in *OR37A-E* genes within the conserved *TAATTGGAT* sequence (motif block I in Hoppe et al., 2000) and in mouse and human *P3* and *P4* putative promoter regions (Lane et al., 2001). Notably, we find a combination of an O/E-like site with a putative homeodomain binding site in *MOR23*, *M71*, and *M72* (mouse, rat, human), in the *OR37* family (mouse), as well as in the zebrafish *OR2.1* gene, the only non-mouse OR gene for which transgenic data exist. The two elements display a typical spacing of 37 bp for both *MOR23* and *M71*, and of a range of 15 to 77 bp in 12 genes studied and are located in the immediate vicinity of the TSS. Conservation of these combined motifs from zebrafish to human is striking. They may represent an essential component of the *cis*-elements regulating OR gene choice and/or expression. Note that the deletion breakpoint in the nonexpressing Tg5′Δ construct is located between these two sites.

We found an additional combination of a homeodo-

main binding and an O/E-like site within intron 2 of *MOR23*, possibly representing an alternate promoter. Suggestive experimental evidence for an alternate promoter in *MOR23* comes from a line that carries a truncation in its single transgene copy from its 5′ end up to a breakpoint located upstream of these motifs in intron 2 and which shows labeled OSNs and glomerular convergence (data not shown). A distinct alternate TSS in *MOR23*, located in exon 2, has been described in the BALB/c mouse strain (Asai et al., 1996). Thus, the *MOR23* gene could have multiple TSS.

Zonal Patterning

Zonal restriction of expression is a not a robust phenotype, as it is altered in a fraction of our transgenic lines. When regulatory interactions are perturbed, particularly as transgenes get smaller (TgΔΔ and Tg3′Δ) and increasingly prone to position effects from flanking genomic sequences, the pattern may default to ventrally extended expression. Moreover, aberrant recombination of transgene copies may perturb zonal patterning by affecting the spacing and/or order of regulatory elements present in the transgene. The shortest transgene able to display correct zonal expression is TgΔ, with 4.9 kb of spliced genomic sequence. Our deletion series of *MOR23* transgenes does not however allow to assign unambiguously specific transgene DNA intervals to zonal control of expression. This is because even the longest constructs able of correct expression can exhibit alterations of zonal expression in a fraction of the lines harboring the construct. The ES route of transgenesis may be superior in this respect, as it permits preselection of transgenes for copy number and integrity. Indeed, none of the three expressing ES-derived strains that were screened for an intact single copy of the SN transgene showed aberrant zonal expression.

The presence of transgene-expressing OSNs in aberrant epithelial zones correlates with the occurrence of ectopic glomeruli. Thus, in TgΔΔ-7 mice, *MOR23* transgene-expressing OSNs that project medially are distributed within three zones (4, 3, and 2), and three glomeruli are consistently observed on the medial olfactory bulb, with the most dorsal being the MOR23 cognate glomerulus, and two progressively more ventral, ectopic glomeruli. The three glomeruli are likely to be the discrete convergence loci of axons originating from the three individual zones. Supporting this interpretation, the dorsal-most glomeruli reside in the OCAM-negative region of the bulb (zone 4 origin), whereas the two more ventral glomeruli reside in the OCAM-positive region (zones 3 and 2). Further evidence is provided by a correlation between the absolute number of labeled neurons located within the endogenous or ectopic zone and the size of the corresponding glomerulus (data not shown). Together, these observations suggest a code of connectivity in which the association of an expressed OR with an expression zone dictates discrete glomerular projections. Zone boundaries may correlate with differences in gene expression that affect axon guidance, creating distinct projection units. Moreover, we observe that for a particular transgene that is expressed in multiple zones, as MOR23-TgΔΔ-7 or M71-TgD, the corresponding multiple glomeruli maintain similar anteroposterior positions, as seen both on the medial and lateral sides of the bulb.

Role of ORs in Axon Guidance

We made the unexpected observation for both the *MOR23* and *M71* genes that the introduction of a novel transgenic member to the OR gene repertoire can alter the projections of OSNs expressing the cognate endogenous gene. In TgΔΔ-7 bulbs with additional MOR23 glomeruli, a fraction of the axons of OSNs expressing the endogenous *MOR23* gene are seen coursing along the same routes as the axons of transgene-expressing OSNs and innervate the ectopic glomeruli. Similarly, ectopic glomeruli formed by OSNs expressing the M71-TgD transgene are often innervated by axons of OSNs expressing the endogenous *M71* gene. This apparent axonal rerouting is consistent with evidence that OR expression codetermines the position of glomerular targets in the bulb (Mombaerts et al., 1996; Wang et al., 1998). At least two, non-mutually exclusive scenarios can be proposed to interpret these observations. First, axons from endogenous *MOR23*-expressing OSNs, located in zone 4, may be rerouted at the level of the bulb by interactions with axons of *MOR23* transgene-expressing OSNs converging to ectopic glomeruli. Second, mice typically carry a minor population of endogenous *MOR23*-expressing OSNs misplaced within ectopic zones of the epithelium. This misplacement may be incompatible with projection of their axons to the correct domain of the bulb and innervation of the cognate glomeruli, and as a consequence these cells die. However, in transgenic mice with OSNs expressing the same receptor in these ectopic zones and forming ectopic glomeruli, they have now the opportunity to innervate MOR23-type glomeruli, allowing for their survival (Ebrahimi and Chess, 2000). In this model, what appears as rerouting is rather a stabilization of a normally minor population of OSNs.

Both models can be explained by invoking that growth cones of OSNs interact with axons of OSNs expressing the same OR and that these interactions influence their navigation or survival. These homotypic interactions could involve the OR protein itself. We have shown that extended expression of a transgenic OR throughout several zones of the epithelium is accompanied by a pattern of discrete projections to as many glomeruli. This argues for the existence of relatively tight boundaries between zones that dictate a pattern of zone-to-zone projections between olfactory epithelium and bulb (Yoshihara et al., 1997). However, some degree of cross-zone axonal projections driven by OR homotypic interactions may take place. Thus, OSN axonal connectivity may be more plastic than originally suspected, and one contributing force may be OR homotypic interactions.

Experimental Procedures

Rapid Amplification of 5′ cDNA Ends

For *MOR23*: 2 μg total RNA from olfactory mucosa of 2-week-old mice of the C57BL/6J strain was reverse transcribed using the *MOR23*-specific reverse primer *TSP-1* (Asai et al., 1996). T4 RNA-ligase was used to ligate an anchor oligonucleotide to the 3′ end of the first strand cDNA. Two rounds of nested PCR using TSP-2 and TSP-3 reverse primers (Asai et al., 1996), respectively, generated

products that were directly sequenced or subcloned into pGEM-T. The cDNA sequences were compared with genomic sequences (GenBank X92969).

For *M71*: RNA from 2-week-old mice of the 129/SvEv strain (Taconic) was reverse transcribed and the cDNA amplified using the SMART kit (Clontech). For *M72*, the same procedure was used on RNA from C57BL/6J mice.

MOR23 Targeting Vectors and Transgenes

A 9.4 kb SacI-NheI fragment containing *MOR23* was subcloned from a P1 phage (129/Sv strain) into pBluescript. A PacI site was engineered three nucleotides downstream of the stop codon, to produce plasmid *MOR23/Pac*. Three targeting constructs were derived from this plasmid. The *neo*-selectable gene (*LNL*) was removed from the targeted and ES-Tg loci by crossing mice with *EIIa-Cre* transgenic mice (Lakso et al., 1996). Analyses were performed with mice in a mixed 129 × C57BL/6J background that did not carry the *Cre* transgene.

For ES-Tg-I, -II, and -III, genomic transgene integration sites were mapped by inverse PCR and mapping of polymorphisms using B6 × spretus backcross mapping panels (Jackson Laboratories) or by DNA-FISH. Chromosomal locations are 5G3 (145.02 Mb) for ES-Tg-I; 2D (86.00 Mb) for ES-Tg-II; and 10A2 for ES-Tg-III. The *MOR23* gene resides at 1H3 (165.03 Mb).

Five transgenes for pronuclear microinjection were derived from plasmid *MOR23/Pac*. TgSN was constructed by ligating an *IRES-taulacZ* fragment. For TgΔ, the sequence of the second intron (3478 to 8018 in GenBank X92969) was excised from plasmid *MOR23/PacI* to create plasmid *TgΔ/Pac*, and *IRES-taulacZ* was inserted. For Tg$\Delta\Delta$, the sequence of the first intron (1772 to 3128) was excised from plasmid *TgΔ/Pac*, and *IRES-taulacZ* was inserted. For Tg3′Δ, the BsaI to NheI (9263 to 10,663) fragment of Tg$\Delta\Delta$ was excised. For Tg5′Δ, a XhoI site was introduced at position −10 (1608) from the TSS in Tg$\Delta\Delta$ and the SacI (1213) to XhoI fragment was deleted. DNA was microinjected into F2(C57BL/6J × CBA) zygotes.

M71 Targeting Vectors and Transgenes

M71 gene targeting has been described (Bozza et al., 2002). The plasmid *M71/Pac* consists of a 9.2 kb genomic fragment containing *M71* with a PacI site engineered three nucleotides downstream of the stop codon. For the targeted mutations, a PacI cassette containing *IRES-taulacZ-LTNL* or *IRES-tauGFP-LTNL* was inserted. The *tk-neo*-selectable markers were removed by Cre-mediated recombination in ES cells. Mice are in a mixed 129 × C57BL/6J background. For the *M71* transgene, *IRES-taulacZ* was inserted into the PacI site of *M71/PacI*. Founders were bred to 129/SvEv mice.

Assays for β-Galactosidase Activity in Whole-Mount Specimens

Indigogenic histochemistry with Xgal as a substrate was performed as described (Mombaerts et al., 1996). For fluorescent detection of β-galactosidase activity, unfixed whole-mount specimens were exposed for 2 min to Xgal (0.2 mg/ml) and the dye Fast Red Violet LB (1 mg/ml) (Mohler and Blau, 1996) and imaged on a Zeiss LSM 510 confocal microscope.

Histological Analysis of Tissue Sections

For immunostaining, tissues were fixed in 2% formaldehyde, 13.5 mg/ml lysine, 2.1 mg/ml sodium periodate, and 0.1 M sodium phosphate buffer at pH 7.4 on ice for 2 hr and frozen in OCT. An anti-β-galactosidase rabbit IgG fraction (Cappel) was applied onto coronal sections at a 1:500 dilution, followed by a Texas red-conjugated goat affinity-purified antibody to rabbit IgG (Cappel) at a 1:100 dilution. For NCAM and OCAM stainings, mouse monoclonal antibodies, NCAM-OB11 (Sigma), and RNCAM (BD Transduction Laboratories), respectively, were used. DAPI (Sigma) or TOTO-3 (Molecular Probes) stained nuclei. Sections were examined with a Zeiss Axioplan 2 fluorescence microscope or a Zeiss LSM 510 confocal microscope.

In situ RNA hybridization was performed as described (Strotmann et al., 2000).

Sequence Analysis

Sequences of *OR37* genes (Hoppe et al., 2000) were from AJ251154.1 and AC023789.8. Zebrafish *OR2.1* sequences (Mori et al., 2000) were from AB026133.1. Mouse *M71* and M72 sequences were obtained from BAC 86i21 (Research Genetics) of 129/SvJ origin; we deposited them as AF281061 and AF247656, respectively. Rat *M71* and *M72* sequences were obtained from RPCI-32 BAC 224c14. Rat *OR23* was subcloned and sequenced from RPCI-32 BAC 127i10. There appears to be only one human ortholog to mouse *M71* and *M72*, which we term human *M72*; it was obtained by subcloning and sequencing from BAC 210L3 (Genome Systems). Human *OR23* was obtained from public databases.

Searches for short, gapless, multiply repeated motifs were performed using Consensus v6c (Stormo and Hartzell, 1989) and Gibbs Sampler (Lawrence et al., 1993) packages with default general parameter settings, after masking of simple genomic repeats. Gapped multiple alignments were performed using ClustalW (Thompson et al., 1994), with manual adjustments. The degenerate letter code for nucleotide bases is as follows: H = A, C, or T; M = A or C; R = A or G; V = A, C, or G; Y = C or T.

Acknowledgments

Technical support was provided by Alicia Beeghly, Kristina Hedbacker, Mai Mok, and Irina Tserlyuk. Chimeric and transgenic mice were produced by Ruben Peraza and Ning Wang from the Transgenic Service at The Rockefeller University. We thank Ivan Rodriguez for advice. Jim Darnell, Bill Dreyer, Denis Duboule, Sam Pfaff, Sid Strickland, Lubert Stryer, and Pierre Vassalli provided useful comments on an early version of the manuscript. Postdoctoral fellowship support to A.V. was from the Roche Research Foundation, the Swiss National Foundation, and the Norman and Rosita Winston Foundation; to A.R. from the National Institutes of Health; to P.F. from Bristol-Myers-Squibb, NIH, and the Kirby Center of Sensory Neuroscience at The Rockefeller University; and to M.Z. from the Burroughs Wellcome Fund. P.M. acknowledges grant support from NIH.

Received: September 17, 2001
Revised: May 28, 2002

References

Asai, H., Kasai, H., Matsuda, Y., Yamazaki, N., Nagawa, F., Sakano, H., and Tsuboi, A. (1996). Genomic structure and transcription of a murine odorant receptor gene: differential initiation of transcription in the olfactory and testicular cells. Biochem. Biophys. Res. Commun. *221*, 240–247.

Bozza, T., Feinstein, P., Zheng, C., and Mombaerts, P. (2002). Odorant receptor expression defines functional units in the mouse olfactory system. J. Neurosci. *22*, 3033–3043.

Buck, L.B. (2000). The molecular architecture of odor and pheromone sensing in mammals. Cell *100*, 611–618.

Buck, L., and Axel, R. (1991). A novel multigene family may encode odorant receptors: a molecular basis for odor recognition. Cell *65*, 175–187.

Bulger, M., Bender, M.A., van Doorninck, J.H., Wertman, B., Farrell, C.M., Felsenfeld, G., Groudine, M., and Hardison, R. (2000). Comparative structural and functional analysis of the olfactory receptor genes flanking the human and mouse β-globin gene clusters. Proc. Natl. Acad. Sci. USA *97*, 14560–14565.

Chess, A., Simon, I., Cedar, H., and Axel, R. (1994). Allelic inactivation regulates olfactory receptor gene expression. Cell *78*, 823–834.

Dugas, J.C., and Ngai, J. (2001). Analysis and characterization of an odorant receptor gene cluster in the zebrafish genome. Genomics *71*, 53–65.

Ebrahimi, F.A., and Chess, A. (2000). Olfactory neurons are interdependent in maintaining axonal projections. Curr. Biol. *10*, 219–222.

Ebrahimi, F.A., Edmondson, J., Rothstein, R., and Chess, A. (2000). YAC transgene-mediated olfactory receptor gene choice. Dev. Dyn. *217*, 225–231.

Hoppe, R., Weimer, M., Beck, A., Breer, H., and Strotmann, J. (2000). Sequence analyses of the olfactory receptor gene cluster *mOR37* on mouse chromosome 4. Genomics *66*, 284–295.

Ishii, T., Serizawa, T., Kohda, A., Nakatani, H., Shiroishi, T., Okumura, K., Iwakura, Y., Nagawa, F., Tsuboi, A., and Sakano, H. (2001). Monoallelic expression of the odourant receptor gene and axonal projection of olfactory sensory neurones. Genes Cells *6*, 71–78.

Lakso, M., Pichel, J.G., Gorman, J.R., Sauer, B., Okamoto, Y., Lee, E., Alt, F.W., and Westphal, H. (1996). Efficient in vivo manipulation of mouse genomic sequences at the zygote stage. Proc. Natl. Acad. Sci. USA *93*, 5860–5865.

Lane, R.P., Cutforth, T., Young, J., Athanasio, M., Friedman, C., Rowen, L., Evans, G., Axel, R., Hood, L., and Trask, B.J. (2001). Genomic analysis of orthologous mouse and human olfactory receptor loci. Proc. Natl. Acad. Sci. USA *98*, 7390–7395.

Lawrence, C.E., Altschul, S.F., Boguski, M.S., Liu, J.S., Neuwald, A.F., and Wootton, J.C. (1993). Detecting subtle sequence signals: a Gibbs sampling strategy for multiple alignment. Science *262*, 208–214.

Malnic, B., Hirono, J., Sato, T., and Buck, L.B. (1999). Combinatorial receptor codes for odors. Cell *96*, 713–723.

Mann, R.S. (1995). The specificity of homeotic gene function. Bioessays *17*, 855–863.

Mohler, W.A., and Blau, H.M. (1996). Gene expression and cell fusion analyzed by *lacZ* complementation in mammalian cells. Proc. Natl. Acad. Sci. USA *93*, 12423–12427.

Mombaerts, P. (2001a). The human repertoire of odorant receptor genes and pseudogenes. Annu. Rev. Genomics Hum. Genet. *2*, 493–510.

Mombaerts, P. (2001b). How smell develops. Nat. Neurosci. *4*, 1192–1198.

Mombaerts, P., Wang, F., Dulac, C., Chao, S.K., Nemes, A., Mendelsohn, M., Edmondson, J., and Axel, R. (1996). Visualizing an olfactory sensory map. Cell *87*, 675–686.

Mori, T., Sakai, M., Matsuoka, I., and Kurihara, K. (2000). Analysis of promoter activity of 5′-upstream regions of zebrafish olfactory receptor genes. Biol. Pharm. Bull. *23*, 165–173.

Nagao, H., Yoshihara, Y., Mitsui, S., Fujisawa, H., and Mori, K. (2000). Two mirror-image sensory maps with domain organization in the mouse main olfactory bulb. Neuroreport *11*, 3023–3027.

Pyrski, M., Xu, Z., Walters, E., Gilbert, D.J., Jenkins, N.A., Copeland, N.G., and Margolis, F.L. (2001). The OMP-lacZ transgene mimics the unusual expression pattern of OR-Z6, a new odorant receptor gene on mouse chromosome 6: implication for locus-dependent gene expression. J. Neurosci. *21*, 4637–4648.

Qasba, P., and Reed, R.R. (1998). Tissue and zonal-specific expression of an olfactory receptor transgene. J. Neurosci. *18*, 227–236.

Ressler, K.J., Sullivan, S.L., and Buck, L.B. (1993). A zonal organization of odorant receptor gene expression in the olfactory epithelium. Cell *73*, 597–609.

Ressler, K.J., Sullivan, S.L., and Buck, L.B. (1994). Information coding in the olfactory system: evidence for a stereotyped and highly organized epitope map in the olfactory bulb. Cell *79*, 1245–1255.

Rodriguez, I., Feinstein, P., and Mombaerts, P. (1999). Variable patterns of axonal projections of sensory neurons in the mouse vomeronasal system. Cell *97*, 199–208.

Serizawa, S., Ishii, T., Nakatani, H., Tsuboi, A., Nagawa, F., Asano, M., Sudo, K., Sakagami, J., Sakano, H., Ijiri, T., et al. (2000). Mutually exclusive expression of odorant receptor transgenes. Nat. Neurosci. *3*, 687–693.

Sosinsky, A., Glusman, G., and Lancet, D. (2000). The genomic structure of human olfactory receptor genes. Genomics *70*, 49–61.

Stormo, G.D., and Hartzell, G.W. (1989). Identifying protein-binding sites from unaligned DNA fragments. Proc. Natl. Acad. Sci. USA *86*, 1183–1187.

Strotmann, J., Conzelmann, S., Beck, A., Feinstein, P., Breer, H., and Mombaerts, P. (2000). Local permutations in the glomerular array of the mouse olfactory bulb. J. Neurosci. *20*, 6927–6938.

Sullivan, S.L., Adamson, M.C., Ressler, K.J., Kozak, C.A., and Buck, L.B. (1996). The chromosomal distribution of mouse odorant receptor genes. Proc. Natl. Acad. Sci. USA *93*, 884–888.

Thompson, J.D., Higgins, D.G., and Gibson, T.J. (1994). CLUSTAL W: improving the sensitivity of progressive multiple sequence alignment through sequence weighting, positions-specific gap penalties and weight matrix choice. Nucleic Acids Res. *22*, 4673–4680.

Touhara, K., Sengoku, S., Inaki, K., Tsuboi, A., Hirono, J., Sato, T., Sakano, H., and Haga, T. (1999). Functional identification and reconstitution of an odorant receptor in single olfactory neurons. Proc. Natl. Acad. Sci. USA *96*, 4040–4045.

Tsuboi, A., Yoshihara, S., Yamazaki, N., Kasai, H., Asai-Tsuboi, H., Komatsu, M., Serizawa, S., Ishii, T., Matsuda, Y., Nagawa, F., et al. (1999). Olfactory neurons expressing closely linked and homologous odorant receptor genes tend to project their axons to neighboring glomeruli on the olfactory bulb. J. Neurosci. *19*, 8409–8418.

Vassar, R., Ngai, J., and Axel, R. (1993). Spatial segregation of odorant receptor expression in the mammalian olfactory epithelium. Cell *74*, 309–318.

Vassar, R., Chao, S.K., Sitcheran, R., Nunez, J.M., Vosshall, L.B., and Axel, R. (1994). Topographic organization of sensory projections to the olfactory bulb. Cell *79*, 981–991.

Wang, S.S., Tsai, R.Y., and Reed, R.R. (1997). The characterization of the Olf-1/EBF-like HLH transcription factor family: implications in olfactory gene regulation and neuronal development. J. Neurosci. *17*, 4149–4158.

Wang, F., Nemes, A., Mendelsohn, M., and Axel, R. (1998). Odorant receptors govern the formation of a precise topographic map. Cell *93*, 47–60.

Xie, S.Y., Feinstein, P., and Mombaerts, P. (2000). Characterization of a cluster comprising ~100 odorant receptor genes in mouse. Mamm. Genome *11*, 1070–1078.

Yoshihara, Y., Kawasaki, M., Tamada, A., Fujita, H., Hayashi, H., Kagamiyama, H., and Mori, K. (1997). OCAM: A new member of the neural cell adhesion molecule family related to zone-to-zone projection of olfactory and vomeronasal axons. J. Neurosci. *17*, 5830–5842.

Zhang, X., and Firestein, S. (2002). The olfactory receptor gene superfamily of the mouse. Nat. Neurosci. *5*, 124–133.